Soft Matter

PAPER

View Article Online
View Journal | View Issue

Cite this: *Soft Matter*, 2022, **18**, 1385

Pyridine-functional diblock copolymer nanoparticles synthesized *via* RAFT-mediated polymerization-induced self-assembly: effect of solution pH†

Shang-Pin Wen [a] and Lee A. Fielding *[ab]

Polymerization-induced self-assembly (PISA) *via* reversible addition–fragmentation chain transfer (RAFT) polymerization has become widely recognized as a versatile and efficient strategy to prepare complex block copolymer nanoparticles with controlled morphology, size, and surface functionality. In this article, we report the preparation of cationic sterically-stabilized poly(2-vinylpyridine)-poly(benzyl methacrylate) (P2VP–PBzMA) diblock copolymer nanoparticles *via* RAFT-mediated PISA under aqueous emulsion polymerization conditions. It is demonstrated that the solution pH during PISA has a dramatic effect on the resulting P2VP–PBzMA nanoparticles, as judged by dynamic light scattering (DLS), disc centrifuge photosedimentometry (DCP) and transmission electron microscopy (TEM). Varying the solution pH results in the P2VP stabilizer having different solubilities due to protonation/deprotonation of the pyridine groups. This allows P2VP–PBzMA nanoparticles with tunable diameters to be prepared by altering the DP of the stabilizer (P2VP) and/or core-forming block (PBzMA), or simply by changing the solution pH for a fixed copolymer composition. For example, P2VP–PBzMA nanoparticles with larger diameters can be obtained at higher solution pH as the protonation degree of the P2VP stabilizer has a large effect on both the aggregation of polymer chains during the PISA process, and the resulting behavior of the diblock copolymer nanoparticles. Changing the dispersion pH post-polymerization has a relatively limited effect on particle diameter. Furthermore, aqueous electrophoresis studies indicate that these P2VP–PBzMA nanoparticles had good colloidal stability and high cationic charge (>30 mV) below pH 5 and can be dispersed readily over a wide pH range.

Received 21st December 2021,
Accepted 22nd January 2022

DOI: 10.1039/d1sm01793d

rsc.li/soft-matter-journal

Introduction

In the past two decades, polymerization-induced self-assembly (PISA) *via* reversible addition–fragmentation chain transfer (RAFT) polymerization has attracted significant attention for the preparation of complex block copolymer nanoparticles with tunable morphology, size, and surface functionality.[1–4] PISA has been reported as a versatile and efficient approach to prepare a wide range of diblock copolymer nanoparticles at high solids content without conventional post-polymerization processing techniques.[5,6] This suggests that the RAFT-mediated PISA technique can be potentially utilized for manufacturing mass-produced copolymer products at a low cost.[7] Furthermore, it has been reported that RAFT-mediated PISA can be conducted in various media, such as aqueous,[3,8–12] alcoholic,[13–15] and non-polar solvents.[16–18] During PISA, a solvent-soluble RAFT macromolecular chain transfer agent (macro-CTA) is used as a stabilizer block and chain-extended with a solvent-immiscible or a solvent-miscible monomer to form a second block *via* RAFT emulsion[19,20] or RAFT dispersion[21,22] polymerization, respectively. In comparison to most RAFT dispersion polymerization formulations, RAFT aqueous emulsion polymerization has the advantage of being able to polymerize water-immiscible monomers directly in aqueous conditions. Water is a more environmentally friendly solvent than the typical solvents used in dispersion polymerization formulations and thus negates the use of undesirable volatile organic compounds (VOCs).

Stimulus-responsive polymers include those that can self-assemble, undergo morphology changes, or phase transitions in response to minor external changes in the environment.

[a] *Department of Materials, School of Natural Sciences, University of Manchester, Oxford Road, Manchester, M13 9PL, UK. E-mail: lee.fielding@manchester.ac.uk*
[b] *Henry Royce Institute, The University of Manchester, Oxford Road, Manchester, M13 9PL, UK*

† Electronic supplementary information (ESI) available: ^{1}H NMR spectra of P2VP and P2VP–PBzMA; kinetic studies for the synthesis of $P2VP_{67}$ macro-CTA; solubility of BzMA monomer and P2VP macro-CTAs; additional TEM images for $P2VP_{67}$-$PBzMA_{300}$ nanoparticles; and table detailing the particle diameters, molar masses and molar mass dispersities of the $P2VP_x$–$PBzMA_y$ copolymer particles reported. See DOI: 10.1039/d1sm01793d

These responsive polymers are also named smart, intelligent, or environmentally responsive polymers and can be responsive to numerous stimuli, such as light, solvent, temperature, chemical agents, ionic strength, electrical field, magnetic field, and pH.[23–25] In the past two decades, pH-responsive polymers have attracted great academic and industrial interest as they have a wide-span of potential applications, such as sensors, membranes, chromatography, and drug delivery.[26–28]

pH-stimuli responsive polymers generally have ionizable basic or acidic functional groups, including sulfonic, carboxyl, phosphate, tertiary amines, and pyridine. The ionization of these functional groups depends on solution pH and can affect polymer structure, surface activity, and solubility.[29] Poly(vinyl pyridine)-based block copolymers, *e.g.*, poly(2-vinylpyridine) (P2VP) or poly(4-vinylpyridine) (P4VP), are one of the most widely investigated classes of pH-responsive polymers.[29,30] These polymers typically undergo a phase transition above approximately pH 5, resulting from the deprotonation of pyridine groups.[31,32]

Gohy *et al.* synthesized poly(2-vinylpyridine)-poly((dimethylamino)ethyl methacrylate) diblock copolymers *via* living anionic polymerization, followed by dissolution of copolymers in aqueous solution at differing pH at 1 g L^{-1} to obtain the block copolymer nanoparticles.[33] Armes and coworkers reported poly(ethylene glycol) methacrylate (PEGMA) stabilized P2VP microgels prepared *via* conventional emulsion polymerization in the presence of divinylbenzene (DVB) cross-linker, and demonstrated that these microgels had swelling behavior below pH 4.5.[32,34,35] However, only a few papers reported the successful preparation of poly(vinyl pyridine) related diblock copolymers *via* RAFT polymerization.

Zamfir *et al.* reported the synthesis of polystyrene-poly(2-vinylpyridine) (PS–P2VP) and polystyrene-poly(4-vinylpyridine) (PS–P4VP) *via* RAFT dispersion polymerization using PS macro-CTAs.[36] More extensive side reactions and bimodal molar mass distributions were observed for PS–P4VP diblock copolymers than PS–P2VP copolymers due to the greater reactivity and polarity of 4VP than that of 2VP. Convertine *et al.* demonstrated that the synthesis of P2VP and P4VP macro-CTAs can be achieved *via* bulk RAFT polymerizations using cumyl dithiobenzoate as the CTA in the absence of organic solvents.[37] These macro-CTAs were chain-extended with 4VP or 2VP, and the copolymers had relatively low molar mass distributions, but only low conversions (<40% after polymerization for 6 h) were achieved. Nieswandt *et al.* successfully prepared P2VP–PS and P4VP–PS *via* RAFT aqueous-alcoholic dispersion polymerization using P2VP and P4VP as macro-CTAs, respectively.[38] Copolymers with high molar mass (>100 kg mol^{-1}) could be achieved in both cases, but the P4VP–PS had broader molar mass distributions. Nieswandt *et al.* also reported the preparation of poly(3-vinylpyridine)-poly(styrene) (P3VP–PS) *via* RAFT emulsion polymerization in DMF/H_2O (50/50, v/v) solvent mixtures. P3VP–PS diblock copolymers with narrow molar mass distribution were obtained.[39] However, in all of the reports described above, block copolymer nanoparticles were formed *via* self-assembly of the copolymers in selective solvents. Although, Nieswandt *et al.* claimed that P2VP–PS,[38] P4VP–PS,[38] and P3VP–PS[39] can be successfully prepared *via* RAFT-mediated PISA, they did not investigate these block copolymer nanoparticles directly. Instead, these copolymers were dissolved in THF and precipitated in an excess of ice-cold *n*-hexane to obtain nanoparticles, and the bulk and surface morphologies of the diblock copolymers were investigated. Therefore, to the best of our knowledge, there are no prior reports on the synthesis and direct characterization of poly(vinyl pyridine) related block copolymer nanoparticles prepared *via* RAFT-mediated PISA.

Herein, cationic sterically-stabilized poly(2-vinyl pyridine)-poly(benzyl methacrylate) (P2VP–PBzMA) diblock copolymer nanoparticles were prepared *via* RAFT-mediated PISA under aqueous emulsion polymerization conditions (Scheme 1). Varying the pH of the aqueous continuous phase resulted in the P2VP stabilizer having different solubilities due to protonation/deprotonation of the pyridine groups.[40] This allowed the evaluation of the effect of pH on the formation of P2VP–PBzMA diblock copolymer nanoparticles during PISA. Nanoparticles with tunable diameters were prepared by altering the DP of the stabilizer (P2VP) and/or core-forming block (PBzMA), or simply by changing the solution pH for a fixed copolymer composition. The resulting nanoparticles were characterized using dynamic light scattering (DLS), transmission electron microscopy (TEM), aqueous electrophoresis, and disc centrifuge photosedimentometry (DCP). Additionally, the P2VP–PBzMA diblock copolymers were characterized using nuclear magnetic resonance spectroscopy (NMR) and gel permeation chromatography (GPC). For the sake of brevity, shorthand labels are used throughout this work: P2VP and PBzMA or "V" and "B" are used to denote the two blocks, respectively.

Experimental

Materials

Benzyl methacrylate (BzMA, 98%) and 2-vinylpyridine (2VP, 97%) were purchased from Alfa Aesar (UK) and Sigma-Aldrich (UK), respectively. Monomers were purified to remove inhibitors and impurities before use by passing through a column of activated basic alumina. Diethyl ether (99%), 2,2'-azodiisobutyramidine dihydrochloride (AIBA; 97%), and azobisisobutyronitrile (AIBN, 98%) were purchased from Sigma-Aldrich (UK) and used as received. Tetrahydrofuran (THF, HPLC grade) and ethanol (95%) were purchased from VWR International (UK) and Fisher Scientific (UK), respectively, and both solvents were used as received. Chloroform-d ($CDCl_3$) was purchased from Cambridge Isotope Laboratories (UK). 2-Cyano-2-propyl phenethyl trithiocarbonate (PETTCCP) was prepared in-house using previously published methods.[41,42] Deionized water was obtained from an Elga Purelab Option water purification system.

Preparation of P2VP *via* RAFT solution polymerization in ethanol

In a typical protocol for the synthesis of $P2VP_{25}$ macro-CTA *via* RAFT solution polymerization in ethanol at 15% solids, 2VP (5.7 g, 54.12 mmol), PETTCCP (609.4 mg, 2.17 mmol), AIBN (118.5 mg, 0.72 mmol, PETTCCP/AIBN molar ratio = 3), and ethanol (35.6 g) were weighed into a 100 mL two-necked round-bottom flask equipped with a condenser and a nitrogen inlet.

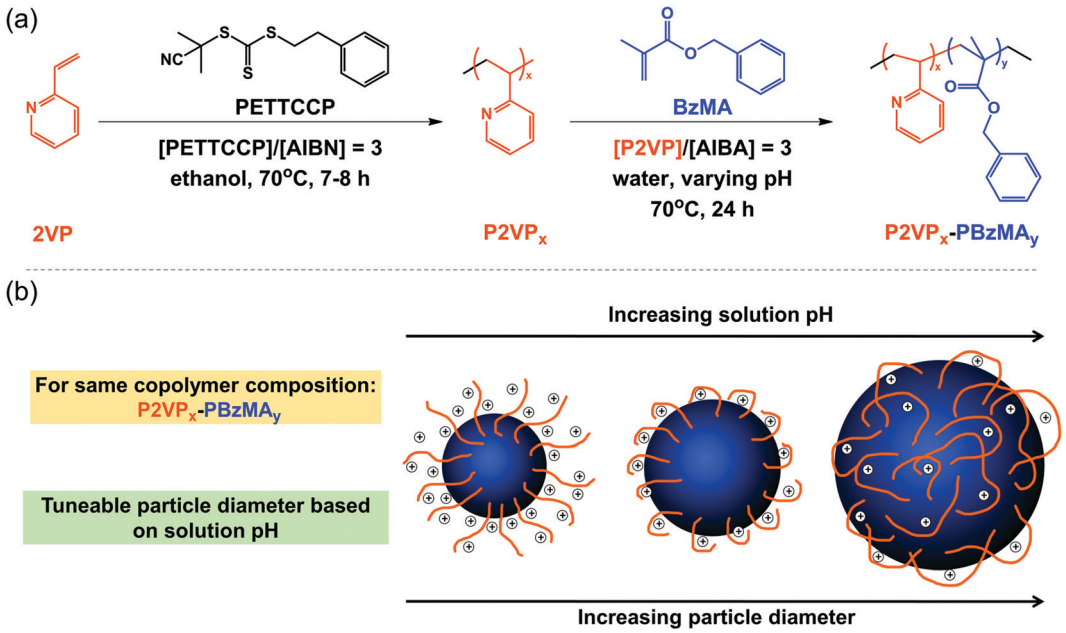

Scheme 1 (a) Synthesis of poly(2-vinylpyridine) (P2VP) macro-CTA *via* RAFT solution polymerization in ethanol at 15% w/w solids, followed by chain-extension with benzyl methacrylate (BzMA) *via* RAFT-mediated PISA at varying pH at 10% w/w solids. (b) Summary of the effect of solution pH on the formation of P2VP–PBzMA diblock copolymer nanoparticles for a fixed target copolymer composition.

The reactor contents were deoxygenated by purging nitrogen for 30 min at ambient temperature. After deoxygenation, the round-bottom flask was immersed into a preheated oil bath at 70 °C, corresponding to time zero of the polymerization. The reaction was heated for 7 hours (or 8 hours for $P2VP_{50}$) and magnetically stirred at 250 rpm. The polymerization was quenched by rapid cooling in an ice bath and exposure to air. The synthesized polymers were precipitated into an excess of cold diethyl ether and collected by three precipitation/decant cycles. The precipitates were further dried under vacuum at 35 °C to obtain a yellow solid of P2VP macro-CTA.

Preparation of P2VP–PBzMA diblock copolymer nanoparticles *via* RAFT aqueous emulsion polymerization

A typical protocol for the preparation of $P2VP_x$–$PBzMA_y$ (V_x–B_y) diblock copolymer nanoparticles *via* RAFT aqueous emulsion polymerization at 10% w/w solids was as follows. For V_{32}–B_{300} synthesized at pH 2, $P2VP_{32}$ macro-CTA (32.3 mg, 0.009 mmol), AIBA (0.8 mg, 0.003 mmol, macro-CTA/AIBA molar ratio = 3), and deionized water were added into a 14 mL vial. The solution pH was slowly adjusted to pH 2 using 0.1 M HCl, and then BzMA (467.7 mg, 2.654 mmol) was added. The solution was purged with N_2 for 10 min prior to immersion in a preheated oil bath set at 70 °C for 24 h. The polymerizations were quenched by exposing to air and cooling to room temperature. Subsequent polymerizations were performed by varying the target copolymer composition and by varying the solution pH from 1.0 to 3.5.

Nuclear magnetic resonance spectroscopy (NMR)

^1H NMR spectra were recorded in $CDCl_3$ using a 400 MHz Bruker Advance III spectrometer with 128 scans being averaged per spectrum.

Gravimetry

Monomer conversions of BzMA for the synthesis of P2VP–PBzMA diblock copolymers were determined *via* gravimetry. Samples (approximately 1.0 g) were withdrawn from the P2VP–PBzMA final dispersions. The specimens were placed in an oven and dried at 60 °C to constant weight. Conversions were calculated from the measured dry residue.

Gel permeation chromatography (GPC)

Molar mass distributions were assessed using a GPC instrument equipped with an Agilent 1260 Infinity pump injection module, an Agilent 1260 Infinity II refractive index detector, and three Phenomenex phenogel columns with a mobile phase of THF at 35 °C. Calibration was achieved using a series of polystyrene standards, ranging from 1×10^3 to 2×10^6 g mol^{-1}. For P2VP homopolymers, samples were dissolved in THF directly prior to GPC analysis. For P2VP–PBzMA diblock copolymers synthesized below pH 4, samples were diluted in deionized water and then titrated to above pH 7 using 0.1 M KOH, and then dried in an oven at 60 °C to remove water. This specific sample preparation procedure led to a decrease in the protonation of P2VP stabilizer and increased the solubility of P2VP–PBzMA diblock copolymers in THF.

Dynamic light scattering (DLS)

Hydrodynamic diameters (D_h) of nanoparticles were recorded using a Malvern Zetasizer Nano ZS instrument at a fixed scattering angle of 173° at 25 °C. DLS samples were prepared by diluting copolymer dispersions to approximately 0.1% w/w using water at pH 2 to minimize potential coagulation. Samples were analyzed using disposable plastic cuvettes and all data were averaged over three consecutive measurements.

Aqueous electrophoresis

Aqueous electrophoresis studies were conducted in disposable folded capillary cells (Malvern DTS1017) using the same Malvern Zetasizer Nano ZS instrument described above. Measurements were performed in the presence of 10^{-3} M KCl as background electrolyte. The solution was initially adjusted to pH 2 using HCl and manually raised to pH 11 by addition of KOH as required. Data were collected at 25 °C and averaged over three consecutive measurements to give the mean zeta potential.

Transmission electron microscopy (TEM)

TEM studies were conducted using a FEI Tecnai G2 20 instrument operating at 200 kV and equipped with a Gatan 1k CCD camera. Aqueous copolymer dispersions were diluted to approximately 0.1% w/w using deionized water at ambient temperature. TEM samples were prepared by depositing 2 μL of diluted copolymer dispersion onto carbon-coated copper grids (Agar Scientific, 400 mesh) and dried under ambient conditions for 30 min. Subsequently, the deposited nanoparticles were stained at ambient temperature in a vapor space above ruthenium tetroxide solution for 7 min[43] prior to TEM analysis to improve image contrast.

Disc centrifuge photosedimentometry (DCP)

DCP studies were conducted using a CPS DC24000 instrument to obtain particle size distributions. The disc centrifuge was operated at 22 000 rpm. The spin fluid contained a density gradient built from 12 to 4% w/w aqueous sucrose, and then 0.5 ml of *n*-dodecane was injected to prevent surface evaporation and to extend the lifetime of the gradient. The aqueous sucrose solutions and diluted samples were adjusted to pH 2, 5, or 9 (as needed) using HCl or KOH before use. Samples (0.1 mL) were injected into the disc for analysis. The disc centrifuge was calibrated using a polystyrene latex standard with a mean particle diameter of 348 nm.

Results and discussion

Synthesis of P2VP macro-CTAs.

RAFT solution polymerization of 2VP was conducted in ethanol at 70 °C (Scheme 1). The polymerizations were quenched at monomer conversions <80% to ensure most of the trithiocarbonate RAFT chain-ends remained intact and minimize bimolecular termination.[44,45] The degree of polymerization (DP) for P2VP macro-CTAs were determined using ^{1}H NMR spectroscopy (Fig. S1, see ESI†) by comparing the integration of proton signals at 8.1–8.6 ppm, corresponding to a proton on the pyridine group of P2VP, with the integration at 3.4–3.5 ppm, corresponding to the two protons on methylene group of the PETTCCP. The calculated DPs for $P2VP_{25}$ and $P2VP_{50}$ macro-CTAs were 32 and 67, respectively.

Fig. 1a and Fig. S2a (ESI†) show the kinetic data for the preparation of $P2VP_{32}$ and $P2VP_{67}$, respectively. The relatively linear conversion/time relationships and the pseudo first-order kinetic plots are reasonably consistent with the features expected for a controlled RAFT polymerization.[17] However, in order to reach approximately 80% conversion, the polymerizations needed to be allow to proceed for at least 7–8 h. This can be attributed to 2-vinylpyridine (2VP) being a type of more-activated monomer (MAM), resulting in the intermediate thiocarbonylthio capped radical species having relatively long half-lives during RAFT polymerisation.[46–49] Therefore, some of the intermediate radical species may be consumed by side reactions or termination, resulting in slower polymerization rates and higher than target DPs of the resulting P2VP macro-CTAs.

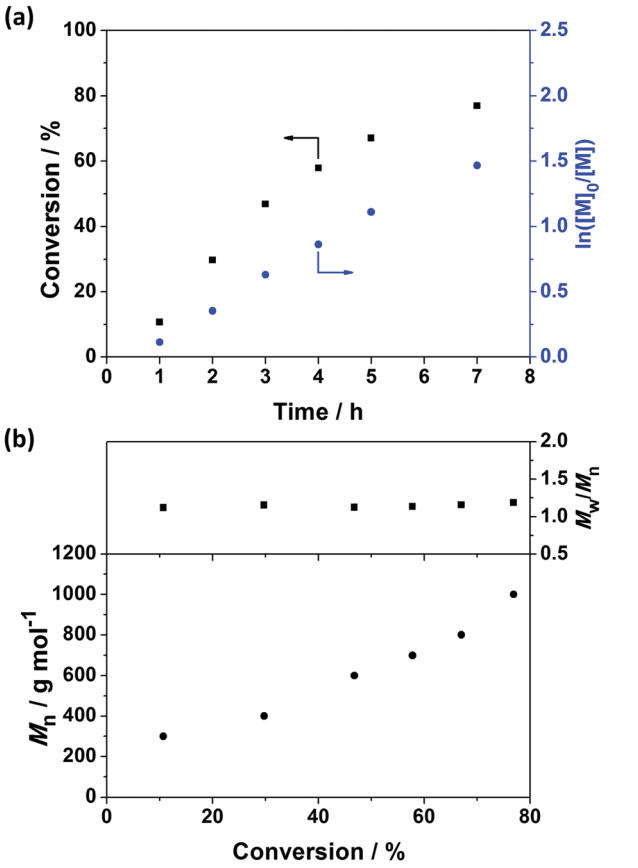

Fig. 1 Kinetic studies for RAFT solution polymerization of 2VP in ethanol: (a) conversion and $\ln([M]_0/[M])$ *versus* reaction time. (b) Evolution of the molar mass (M_n) and molar mass dispersity (M_w/M_n) with monomer conversion. Polymerization conditions: [2VP] : [PETTCCP] : [AIBN] = 75 : 3 : 1, 70 °C, 15% w/w solids.

Fig. 1b and Fig. S2b (see ESI†) show the evolution of the molar mass (M_n) and molar mass dispersity (M_w/M_n) with monomer conversion for $P2VP_{32}$ and $P2VP_{67}$. As the polymerizations progressed, the evolution of molar mass in relation to monomer conversion was close to linear, with relatively narrow molar mass dispersities obtained. However, the molar masses of $P2VP_{32}$ and $P2VP_{67}$ macro-CTAs determined *via* THF GPC analysis were 1200 and 2200 g mol^{-1}, respectively. These values were much lower than the calculated theoretical molar mass, which should be approximately 3600 and 7300 g mol^{-1}, respectively. The low values of molar mass reported by THF GPC analysis were not unexpected and are in good agreement with Nieswandt *et al.*,[38] who prepared P2VP *via* RAFT bulk

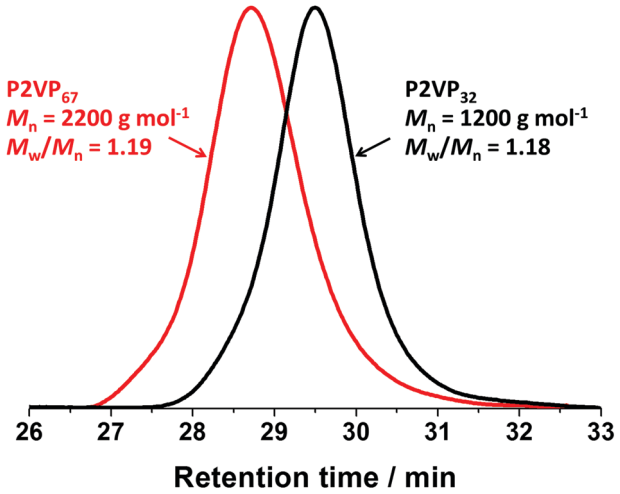

Fig. 2 THF GPC chromatograms obtained for $P2VP_{32}$ and $P2VP_{67}$ macro-CTAs synthesized *via* RAFT solution polymerization in ethanol at 70 °C and 15% w/w solids. Monomer conversions of $P2VP_{32}$ and $P2VP_{67}$ macro-CTAs were 76.9% and 69.6%, respectively.

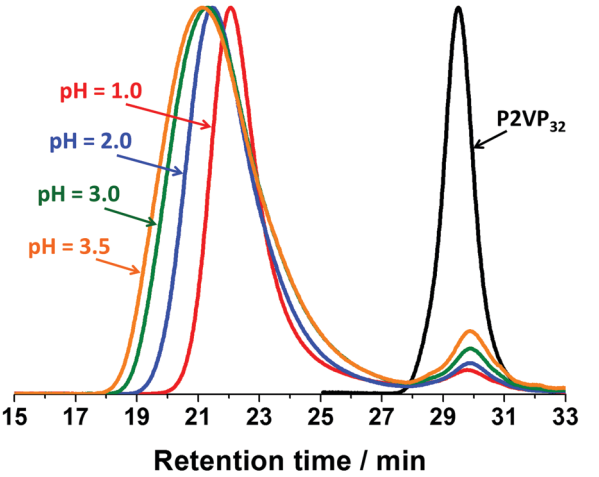

Fig. 3 Representative GPC chromatograms of the $P2VP_{32}$ macro-CTA and $P2VP_{32}$–$PBzMA_{300}$ diblock copolymers synthesized *via* RAFT aqueous emulsion polymerization between pH 1.0 and 3.5.

polymerization and observed obviously smaller GPC M_n values than the theoretical M_n. These deviations from the theoretical M_n values may be partially caused by the differences between the GPC calibration standards (polystyrene) and P2VP, and potentially partially protonated pyridine groups on the P2VP polymer chains. Nevertheless, Fig. 2 shows that the GPC chromatograms of the resulting macro-CTAs were unimodal with relatively narrow molar mass distributions ($M_w/M_n < 1.2$). Given the two P2VP homopolymers underwent relatively well-controlled RAFT polymerization to produce polymers with narrow molar mass distributions, they were utilized as macro-CTAs in the subsequent RAFT emulsion polymerizations using BzMA reported herein.

Characterization of P2VP–PBzMA diblock copolymers.

Cationic sterically-stabilized P2VP–PBzMA diblock copolymer nanoparticles were prepared *via* RAFT-mediated PISA under aqueous emulsion polymerization conditions (Scheme 1). BzMA is insoluble in water, whereas the P2VP stabilizer is soluble in water below pH 4 (Fig. S3, ESI†). Therefore, P2VP–PBzMA diblock copolymers were synthesized using P2VP as a macro-CTA between pH 1.0 and 3.5.

A representative ^{1}H NMR spectrum of a $P2VP_{32}$–$PBzMA_{50}$ diblock copolymer synthesized at pH 2 is shown in Fig. S4 (ESI†). The 2VP and BzMA contents in the diblock copolymer were calculated by comparison of the integration of a proton on pyridine group of P2VP at 8.1–8.6 ppm with the two protons on methylene of PBzMA at 4.5–5.0 ppm. In all cases, the calculated PBzMA DP was higher than target value. This is attributed to a combination of the P2VP chain-ends being 'more-activated', resulting in relatively low chain-extension efficiency,[46] and the presence of a small fraction of 'dead' homopolymer from the synthesis of the macro-CTA.

Fig. 3 shows the GPC chromatograms of the V_{32} macro-CTA and V_{32}–B_{300} diblock copolymers synthesized between pH 1.0 and 3.5. The GPC chromatograms of all the diblock copolymers were successfully shifted to a shorter retention time, indicating that polymers with higher molar mass were obtained. However, the P2VP–PBzMA copolymers had relatively broad molar mass distributions (M_w/M_n) which were mainly a result of tailing towards lower molar mass species (Fig. 3). Furthermore, an obvious low molar mass shoulder at a retention time of 28–32 min was observed in all cases. This shoulder can be attributed to the deactivated P2VP macro-CTA. It is noteworthy that the quantity of the deactivated P2VP macro-CTA decreased with decreasing solution pH, and only limited deactivated P2VP macro-CTA was observed at pH 1. At lower pH, the P2VP macro-CTA will be more ionized as a result of increased protonation of the pyridine groups. This suggested that P2VP macro-CTAs with higher degrees of protonation have better RAFT chain-extension efficiency,[50,51] and there is only a relatively small quantity of 'dead' homopolymer formed during macro-CTA synthesis. Additionally, the GPC traces of the P2VP–PBzMA diblock copolymer at a retention time of 18–27 min show a subtle shift to longer retention time (lower molar mass) with decreasing solution pH. This is consistent with the observation of less 'dead' homopolymer at lower solution pH, and therefore diblock copolymer chains with lower molar mass for a fixed quantity of BzMA monomer.[52,53] In summary, whilst the presence of a minor fraction of P2VP homopolymer is acknowledged, the preparation of P2VP–PBzMA diblock copolymers with relatively well-control molar masses and narrow molar mass distributions (M_w/M_n) can be achieved at low pH.

Self-assembly of P2VP–PBzMA synthesized *via* RAFT-mediated PISA

Fig. S3 (ESI†) shows that the core-forming monomer, BzMA, was insoluble in water, whereas the P2VP stabilizer completely dissolves in water below pH 4.2 and pH 3.8 for $P2VP_{32}$ and $P2VP_{67}$, respectively. This was consistent with the reported pK_a values (3.85–4.75) of related P2VP polymers.[32,54] This confirms

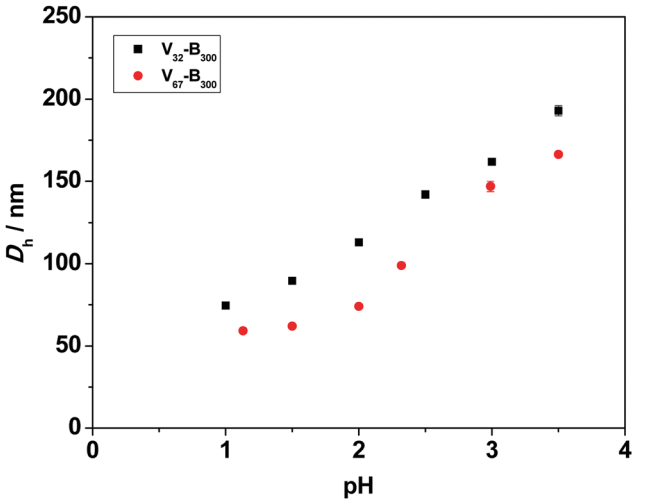

Fig. 4 Mean hydrodynamic diameters (D_h) of $P2VP_x$–$PBzMA_{300}$ (V_x–B_{300}) diblock copolymer nanoparticles prepared *via* RAFT-mediated PISA under aqueous emulsion polymerization conditions at 10% w/w solids and pH 1.0 to 3.5.

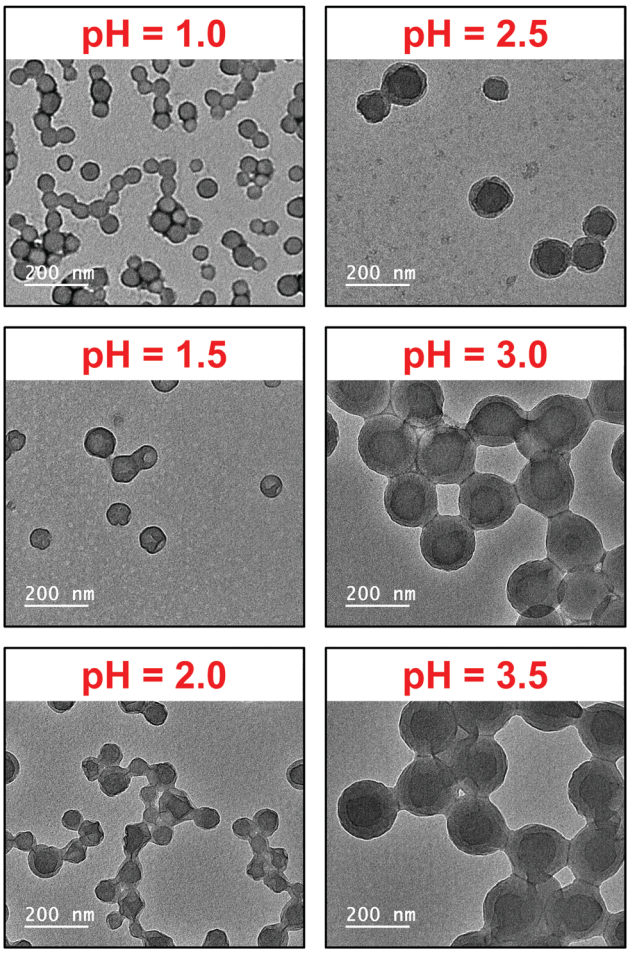

Fig. 5 Representative TEM images for $P2VP_{32}$–$PBzMA_{300}$ (V_{32}-B_{300}) diblock copolymer nanoparticles prepared *via* RAFT aqueous emulsion polymerization of BzMA at 10% w/w solids and pH 1.0 to 3.5.

that the protonation degree of P2VP strongly influences the solubility in water, and longer stabilizers need in more acidic conditions to dissolve.

A series of P2VP–PBzMA (V_x–B_y) diblock copolymer nanoparticles were prepared between pH 1.0 and 3.5. In all cases relatively low particle size dispersities were obtained (Table S1, see ESI†). Fig. 4 shows the mean hydrodynamic diameter (D_h) for a fixed copolymer composition increases as the pH increases from 1.0 to 3.5. For instance, in the V_{67}–B_{300} series, D_h increased from 59 nm at pH 1.0 to 166 nm (approximately three-fold) at pH 3.5. This can be attributed to the P2VP stabilizer having different degrees of ionization (cationic charge) resulting from increased protonation of the pyridine groups at lower solution pH.[55,56] The higher charge of the stabilizer leads to stronger electrostatic repulsion and thus improved stabilization of the resulting nanoparticles.[57] Therefore, at lower solution pH, P2VP–PBzMA nanoparticles with smaller diameters were obtained during PISA. In contrast, the protonation degree of P2VP decreases with increasing solution pH, resulting in weaker electrostatic repulsion and the formation of larger P2VP–PBzMA particles. This indicated that the degree of electrostatic repulsion in the corona (stabilizer) of the forming nanoparticles directly influences the aggregation number of polymeric chains (N_{agg}) which are incorporated into the copolymer nanoparticles and therefore the number of copolymer chains per unit surface area (S_{agg}).[57,58] These observations are similar to the anionic sterically-stabilized poly(potassium 3-sulfopropyl methacrylate) (PKSPMA)–PBzMA nanoparticles, which were prepared *via* RAFT-mediated PISA with a fixed target diblock copolymer composition in various alcohol/water mixtures.[59] These previous results indicated that the repulsive interactions between neighboring anionic PKSPMA stabilizer chains were higher in water-rich solvent mixtures than that in alcohol–rich solvent mixtures. Therefore, the greater electrostatic repulsion between the stabilizer chains led to the self-assembly of PKSPMA–PBzMA chains into particles with comparatively lower aggregation numbers and therefore smaller particle diameters.

For the V_{32}–B_{300} series synthesized with varying solution pH (Fig. 4), the same trend was observed, *i.e.*, the mean hydrodynamic diameter increased with increasing pH. When comparing the two series at a given pH, the V_{32}–B_{300} nanoparticles were consistently larger than the V_{67}–B_{300} particles. This can be attributed to the chain length (DP) of the $P2VP_{32}$ stabilizer being approximately half that of $P2VP_{67}$. Thus, the shorter P2VP stabilizer occupies a lower surface area in the corona of the nanoparticles, allowing more chains to aggregate together (higher N_{agg}) and ultimately form larger particles.[60,61]

Fig. 5 and Fig. S5 (see ESI†) show representative TEM images of the V_x–B_{300} diblock copolymer nanoparticles prepared. Staining with RuO_4 was used to increase the contrast of the copolymer particles (both P2VP and PBzMA blocks).[62] However, the stain is likely to have an affinity to one block over the other, and thus several TEM images appear to have an obvious core–shell morphology. Nevertheless, spherical nanoparticles were obtained in all cases and the mean TEM diameters were generally in agreement with mean hydrodynamic diameter determined by

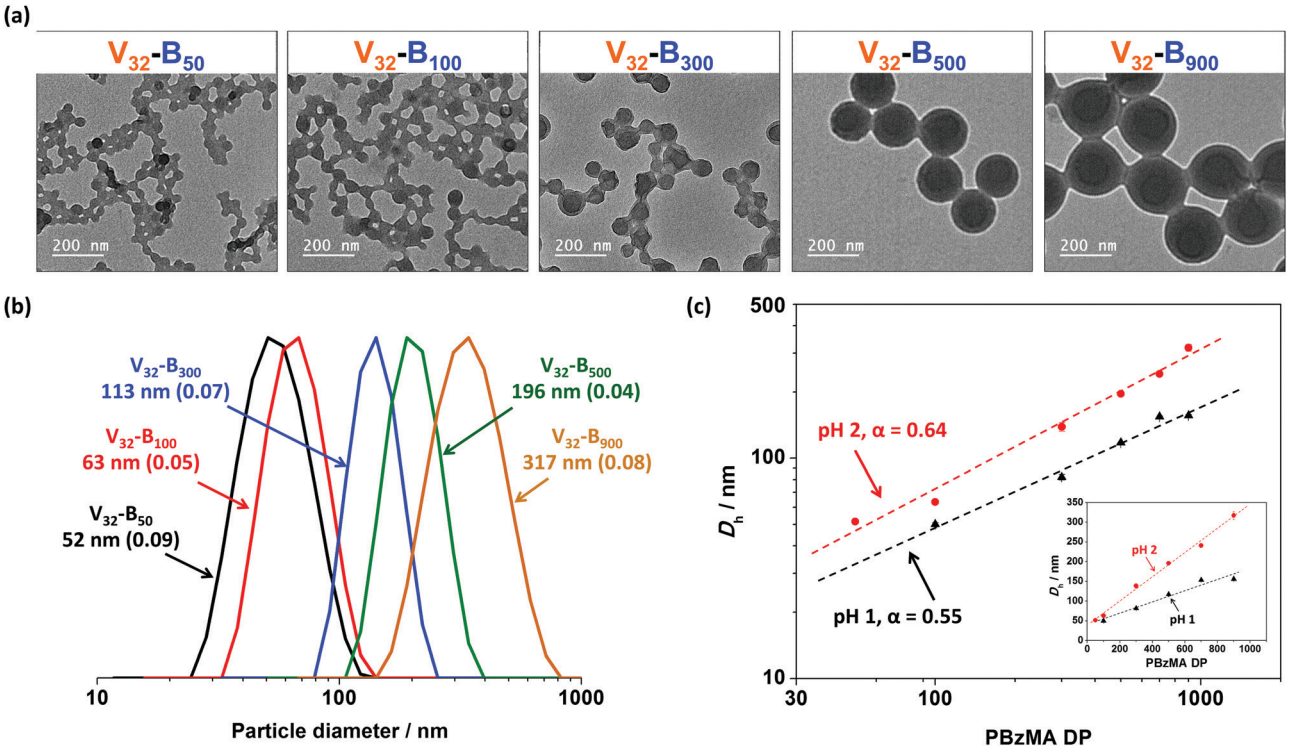

Fig. 6 (a) Representative TEM images for P2VP$_{32}$–PBzMA$_y$ (target y = 50, 100, 300, 500, and 900) nanoparticles synthesized *via* RAFT-mediated PISA under aqueous emulsion polymerization conditions at pH 2 and 10% w/w solids. (b) Corresponding DLS intensity distributions and mean hydrodynamic diameter (DLS polydispersity index in brackets). (c) Double-logarithmic plot for mean hydrodynamic diameter (D_h) *versus* degree of polymerization (DP) of the PBzMA core-forming block for P2VP$_{32}$–PBzMA$_y$ synthesized at pH 1 and pH 2. The inset shows the particle diameter changes using linear scales.

DLS (Fig. 4 and Table S1, see ESI†). The formation of copolymer spheres and not higher order morphologies is consistent with related PISA formulations which used polyelectrolytes as stabilizers, such as P2VP–PS[38] and PKSPMA–PBzMA.[59] This further supports the consensus that strong electrostatic repulsion (either positive or negative charge) between adjacent stabilizer chains inhibits the formation of higher order morphologies, such as worm-like micelles and vesicles.

P2VP–PBzMA diblock copolymer nano-objects with varying PBzMA DP

The mean particle diameters of V$_x$–B$_y$ nano-objects prepared at fixed pH can also be tuned by varying the DP of core-forming PBzMA block. More specifically, the mean hydrodynamic diameters recorded when using a fixed P2VP$_{32}$ macro-CTA increased approximately linearly when increasing the DP of PBzMA from 50 to 900 at both pH 1 and pH 2 (Fig. 6c). For example, in the pH 2 series, the mean hydrodynamic diameter of V$_{32}$–B$_{900}$ (317 nm) was approximately six-fold larger than V$_{32}$–B$_{50}$ (52 nm). Furthermore, particle diameters determined by DLS (Fig. 6b) were consistent with TEM studies (Fig. 6a), which also confirmed a spherical morphology was obtained in all cases. It is noteworthy that the DLS polydispersity index values remained relatively low (<0.1) even when preparing V$_x$–B$_y$ nanoparticles with relatively large core-forming PBzMA blocks (*e.g.* V$_{32}$–B$_{900}$).

The mean hydrodynamic diameter (D_h) increased as a power law of the PBzMA degree of polymerization (DP) and can be described using $D_h = k(DP)^{\alpha}$, where k and α represent a constant and the power law exponent, respectively.[44,63] Fig. 6c shows a double-logarithmic plot of D_h against PBzMA DP for V$_{32}$–B$_y$ (target y = 50, 100, 300, 500, and 900) nanoparticles prepared at pH 1 and pH 2. Both series had a linear relationship with calculated α values of 0.55, and 0.64 for pH 1 and pH 2, respectively. Both α values were close to a value of 2/3, suggesting that configurations of the PBzMA chains are relatively stretched.[44,63,64] It is noteworthy that the value of α at pH 2 was about 16% greater than that at pH 1, indicating that the core-forming PBzMA block was more stretched for particles synthesized at higher solution pH. This supports the observations made in the section above in that at lower pH, the P2VP stabilizer had higher cationic charge. Thus, the greater electrostatic repulsion between the stabilizer chains results in the self-assembly of P2VP–PBzMA chains into particles with comparatively lower aggregation numbers and therefore particle diameters. Furthermore, the effect of electrostatic repulsion generated from the P2VP stabilizer was more obvious with higher target PBzMA DP. Specifically, the particle diameter of V$_{32}$–B$_{50}$ prepared at pH 2 was 4% larger than same composition prepared at pH 1, whereas it was approximately 90% larger when target PBzMA DP was 900.

Colloidal stability of P2VP–PBzMA diblock copolymer nanoparticles

Aqueous electrophoresis and dynamic light scattering data for V$_{32}$–B$_{300}$ nanoparticles (entry 4, Table S1, ESI†) as a function of pH are shown in Fig. 7. The nanoparticles were highly cationic,

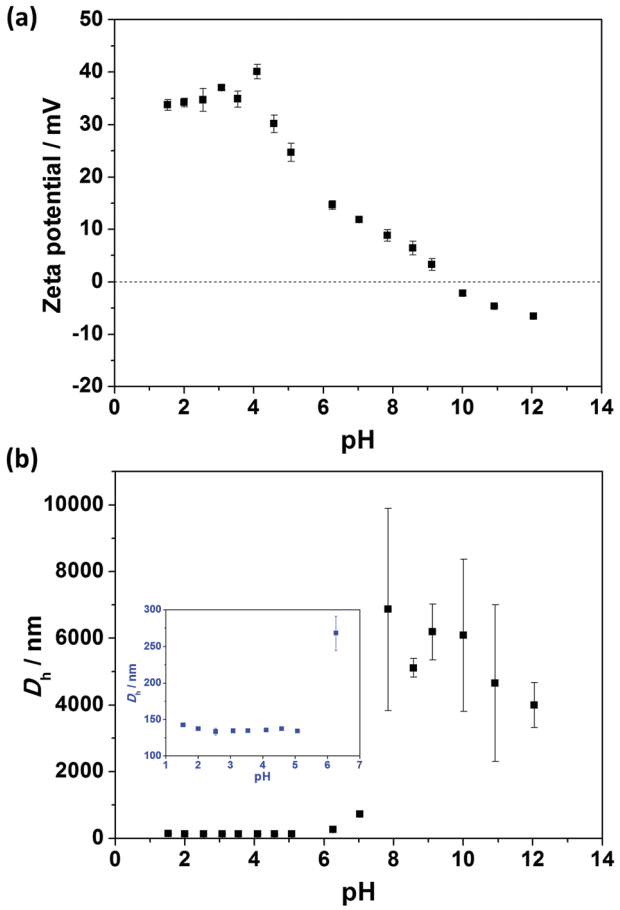

Fig. 7 (a) Aqueous electrophoresis and (b) dynamic light scattering data obtained for $P2VP_{32}$–$PBzMA_{300}$ diblock copolymer nanoparticles synthesized *via* RAFT-mediated PISA under aqueous emulsion polymerization conditions at pH 2.5 (entry 4, Table S1, ESI†). Measurements were conducted using 1 mM KCl as a background electrolyte. The solution pH was initially adjusted to pH 1.5 by the addition of HCl and subsequently manually titrated to pH 12 using KOH. The inset shows a magnification of the particle diameter below pH 7.

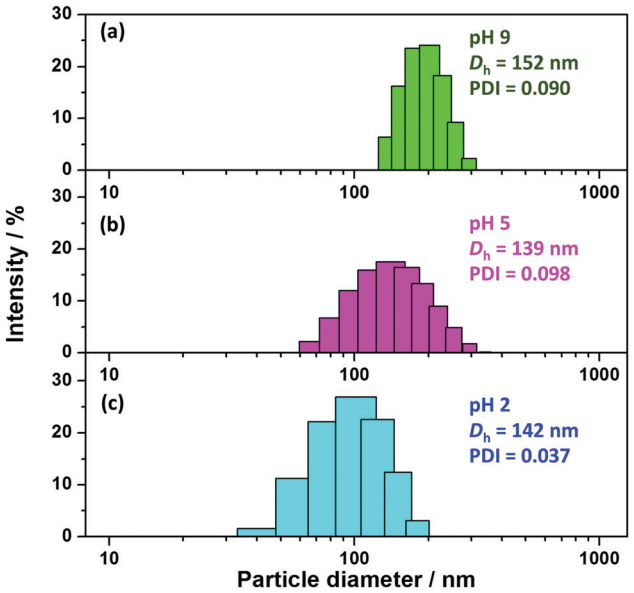

Fig. 8 DLS histograms of $PV2P_{32}$–$PBzMA_{300}$ diblock copolymer nanoparticles prepared *via* RAFT-mediated PISA at 70 °C and pH 2.5 (entry 4, Table S1, ESI†) and dispersed in deionized water adjusted to (a) pH 9, (b) pH 5, and (C) pH 2 in the absence of KCl electrolyte. The polymer concentration was approximately 0.1% w/w.

with a zeta potential higher than +30 mV below pH 4.5 (Fig. 7a). This can be attributed to the highly protonated pyridine functional groups in acidic conditions. As the pH was increased by the addition of KOH, the zeta potential decreased as a result of partial neutralization of the pyridine groups in this pH range.[65] Furthermore, negative zeta potentials were recorded above the isoelectric point at pH ~9 and reached −7 mV at pH 12 (Fig. 7a). It is not definitively known why negative zeta potentials occur for these particles, but this is often seen in the literature and is reported to result from the adsorption of OH^- ions on the primarily uncharged surface.[66–68] Similar observations were found for the other nanoparticles with longer P2VP stabilizer (*e.g.* V_{67}–B_{300}).

Fig. 7b shows that V_x–B_y diblock copolymer nanoparticles had relatively pH-independent size behavior at low pH (~130 nm <pH 5). The lack of particle swelling or dissolution at low pH further confirms that the cationic P2VP block forms the particle coronas, while the hydrophobic PBzMA block forms the particle cores. In contrast, flocculation occurred above pH 5 as a result of P2VP chain collapse above its pK_a (reported pK_a 3.85–4.75 for P2VP latexes[32]) and relatively low zeta potential (zeta potential <18 mV).

It is noteworthy that 1 mM KCl was added as background electrolyte to obtain reliable zeta potential values during the analysis of the V_x–B_y nanoparticles. Furthermore, the dilute dispersion was titrated to approximately pH 1.5 using HCl to maintain protonation of the pyridine groups at the start of the analysis, and the pH was increased by adding KOH. However, high ionic strengths (due to the addition of K^+ and Cl^-) can screen electrostatic interactions between nanoparticles, leading to lower electrostatic repulsion and inducing flocculation.[69,70] In order to investigate the effects of ionic strength on the flocculation of P2VP–PBzMA nanoparticles at varying pH, V_{32}–B_{300} diblock copolymer nanoparticles (entry 4, Table S1, ESI†) were directly dispersed in deionized water adjusted to pH 2.0, 5.0, and 9.0 using HCl or KOH, but without the addition of KCl electrolyte.

The DLS histograms (Fig. 8) show monomodal distributions in all cases, but relatively high DLS polydispersity index values were observed for nanoparticles dispersed in water at pH 5 and pH 9. Furthermore, the percentage of particles with larger size increased with increasing solution pH, indicating that flocculation still occurred to some extent above pH 5. However, the mean hydrodynamic diameter only increased slightly from 142 nm at pH 2 to 152 nm at pH 9, whereas the values reported by in the presence of KCl electrolyte are indicative of highly flocculated dispersions (Fig. 7b).

Fig. 9 shows particle size distributions obtained by disc centrifuge photosedimentometry (DCP) for $P2VP_{32}$–$PBzMA_{300}$ nanoparticles (entry 4, Table S1, ESI†) directly dispersed in

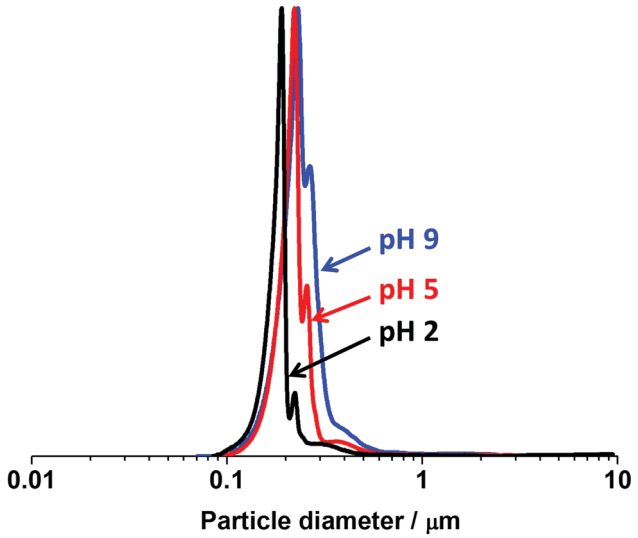

Fig. 9 DCP particle size distributions obtained for $PV2P_{32}$–$PBzMA_{300}$ diblock copolymer nanoparticles prepared *via* RAFT-mediated PISA at 70 °C and pH 2.5 (entry 4, Table S1, ESI†) and dispersed in deionized water adjusted to pH 2, 5, and 9 in the absence of KCl electrolyte. The density of the P2VP–PBzMA particles used for these DCP measurements was taken to be 1.18 g cm^{-3}.

water adjusted to pH 2, 5, and 9 (*i.e.* in the absence of KCl electrolyte). As expected for these samples, only minor flocculation was observed (as indicated by the increasing area of the main peak and shoulder) and the mean weight average diameters were 244, 261 and 303 nm at pH 2, 5 and 9, respectively. Therefore, both DLS and DCP analysis indicated that P2VP–PBzMA nanoparticles can be well-dispersed over a wide pH range, as long at the ionic strength is kept low.

Conclusions

A series of $P2VP_x$–$PBzMA_y$ diblock copolymer nanoparticles were prepared *via* RAFT-mediated PISA under emulsion polymerization conditions. Nanoparticles with tuneable diameters were prepared by changing the copolymer composition, or simply by altering the solution pH for a fixed composition. Generally, nanoparticles with smaller diameters were prepared at lower pHs due to greater electrostatic repulsion between the P2VP stabilizer chains. Thus, the degree of protonation of the P2VP stabiliser directly affects the ease of copolymer aggregation during the PISA process.

The prepared $P2VP_x$–$PBzMA_y$ nanoparticles had good colloidal stability and highly cationic zeta potentials (>30 mV) below pH 5. However, above pH 5 P2VP is not charged, and, with moderate ionic strength (0.1 mM KCl), significant flocculation was observed. Nonetheless, when these nanoparticles were directly dispersed in solutions in the absence of background electrolyte, only negligible flocculation and changes to nanoparticle diameter were observed even at pH 9.

This highly robust synthetic method affords the capability to prepare a desired particle diameter with varying copolymer compositions, or to obtain a favored target copolymer composition with different particle sizes. The capability of these pyridine-functional, cationic, diblock copolymer nanoparticles to be dispersed over a wide pH range whilst maintaining good colloidal stability is promising for applications in future studies.

Conflicts of interest

There are no conflicts to declare.

Acknowledgements

The National Chung-Shan Institute of Science and Technology (NCSIST) is thanked for sponsorship of a PhD studentship for SPW. The University of Manchester Electron Microscopy Centre is acknowledged for access to electron microscopy facilities. This work was supported by the Henry Royce Institute for Advanced Materials, funded through EPSRC grants EP/R00661X/1, EP/S019367/1, EP/P025021/1 and EP/P025498/1.

Notes and references

1 B. Charleux, G. Delaittre, J. Rieger and F. D'Agosto, *Macromolecules*, 2012, **45**, 6753–6765.
2 M. J. Derry, L. A. Fielding and S. P. Armes, *Prog. Polym. Sci.*, 2016, **52**, 1–18.
3 N. J. Warren and S. P. Armes, *J. Am. Chem. Soc.*, 2014, **136**, 10174–10185.
4 F. d'Agosto, J. Rieger and M. Lansalot, *Angew. Chem., Int. Ed.*, 2020, **59**, 8368–8392.
5 X. Zhang, S. Boisse, W. Zhang, P. Beaunier, F. D'Agosto, J. Rieger and B. Charleux, *Macromolecules*, 2011, **44**, 4149–4158.
6 W. Zhang, F. D'Agosto, O. Boyron, J. Rieger and B. Charleux, *Macromolecules*, 2012, **45**, 4075–4084.
7 M. J. Derry, L. A. Fielding and S. P. Armes, *Polym. Chem.*, 2015, **6**, 3054–3062.
8 J. Rieger, C. Grazon, B. Charleux, D. Alaimo and C. Jérôme, *J. Polym. Sci., Part A: Polym. Chem.*, 2009, **47**, 2373–2390.
9 S. Sugihara, A. Blanazs, S. P. Armes, A. J. Ryan and A. L. Lewis, *J. Am. Chem. Soc.*, 2011, **133**, 15707–15713.
10 A. Blanazs, A. Ryan and S. Armes, *Macromolecules*, 2012, **45**, 5099–5107.
11 J. Yeow and C. Boyer, *Adv. Sci.*, 2017, **4**, 1700137.
12 J. Rieger, *Macromol. Rapid Commun.*, 2015, **36**, 1458–1471.
13 W. Cai, W. Wan, C. Hong, C. Huang and C. Pan, *Soft Matter*, 2010, **6**, 5554–5561.
14 M. Semsarilar, E. R. Jones, A. Blanazs and S. P. Armes, *Adv. Mater.*, 2012, **24**, 3378–3382.
15 M. Semsarilar, E. R. Jones and S. P. Armes, *Polym. Chem.*, 2014, **5**, 195–203.
16 L. Houillot, C. Bui, M. Save, B. Charleux, C. Farcet, C. Moire, J.-A. Raust and I. Rodriguez, *Macromolecules*, 2007, **40**, 6500–6509.

17 L. A. Fielding, M. J. Derry, V. Ladmiral, J. Rosselgong, A. M. Rodrigues, L. P. Ratcliffe, S. Sugihara and S. P. Armes, *Chem. Sci.*, 2013, **4**, 2081–2087.
18 L. A. Fielding, J. A. Lane, M. J. Derry, O. O. Mykhaylyk and S. P. Armes, *J. Am. Chem. Soc.*, 2014, **136**, 5790–5798.
19 X. Zhang, J. Rieger and B. Charleux, *Polym. Chem.*, 2012, **3**, 1502–1509.
20 G. Moad, Y. Chong, A. Postma, E. Rizzardo and S. H. Thang, *Polymer*, 2005, **46**, 8458–8468.
21 W.-D. He, X.-L. Sun, W.-M. Wan and C.-Y. Pan, *Macromolecules*, 2011, **44**, 3358–3365.
22 B. Karagoz, L. Esser, H. T. Duong, J. S. Basuki, C. Boyer and T. P. Davis, *Polym. Chem.*, 2014, **5**, 350–355.
23 C. De las Heras Alarcón, S. Pennadam and C. Alexander, *Chem. Soc. Rev.*, 2005, **34**, 276–285.
24 A. E. Smith, X. Xu and C. L. McCormick, *Prog. Polym. Sci.*, 2010, **35**, 45–93.
25 Y. Pei, A. B. Lowe and P. J. Roth, *Macromol. Rapid Commun.*, 2017, **38**, 1600528.
26 J. Hu, G. Zhang, Z. Ge and S. Liu, *Prog. Polym. Sci.*, 2014, **39**, 1096–1143.
27 A. S. Hoffman, *Adv. Drug Delivery Rev.*, 2013, **65**, 10–16.
28 S. Dai, P. Ravi and K. C. Tam, *Soft Matter*, 2008, **4**, 435–449.
29 G. Kocak, C. Tuncer and V. Bütün, *Polym. Chem.*, 2017, **8**, 144–176.
30 S. Förster and M. Antonietti, *Adv. Mater.*, 1998, **10**, 195–217.
31 V. Pinkrah, M. Snowden, J. Mitchell, J. Seidel, B. Chowdhry and G. Fern, *Langmuir*, 2003, **19**, 585–590.
32 D. Dupin, S. Fujii, S. P. Armes, P. Reeve and S. M. Baxter, *Langmuir*, 2006, **22**, 3381–3387.
33 J.-F. Gohy, S. Antoun and R. Jérôme, *Macromolecules*, 2001, **34**, 7435–7440.
34 L. A. Fielding, S. P. Armes, P. Staniland, R. Sayer and I. Tooley, *J. Colloid Interface Sci.*, 2014, **426**, 170–180.
35 J. A. Balmer, E. C. Le Cunff, S. P. Armes, M. W. Murray, K. A. Murray and N. S. Williams, *Langmuir*, 2010, **26**, 13662–13671.
36 M. Zamfir, C. S. Patrickios, F. Montagne, C. Abetz, V. Abetz, L. Oss-Ronen and Y. Talmon, *J. Polym. Sci., Part A: Polym. Chem.*, 2012, **50**, 1636–1644.
37 A. J. Convertine, B. S. Sumerlin, D. B. Thomas, A. B. Lowe and C. L. McCormick, *Macromolecules*, 2003, **36**, 4679–4681.
38 K. Nieswandt, P. Georgopanos and V. Abetz, *Polym. Chem.*, 2021, **12**, 2210–2221.
39 K. Nieswandt, P. Georgopanos, C. Abetz, V. Filiz and V. Abetz, *Materials*, 2019, **12**, 3145.
40 S. Demirci, S. Kinali-Demirci and T. Caykara, *Polymer*, 2013, **54**, 5345–5350.
41 M. Kocik, O. Mykhaylyk and S. Armes, *Soft Matter*, 2014, **10**, 3984–3992.
42 S.-P. Wen, Q. Yue and L. A. Fielding, *Polym. Chem.*, 2021, **12**, 2122–2131.
43 L. A. Fielding, J. A. Lane, M. J. Derry, O. O. Mykhaylyk and S. P. Armes, *J. Am. Chem. Soc.*, 2014, **136**, 5790–5798.
44 S. Förster, M. Zisenis, E. Wenz and M. Antonietti, *J. Chem. Phys.*, 1996, **104**, 9956–9970.
45 D. J. Keddie, *Chem. Soc. Rev.*, 2014, **43**, 496–505.
46 G. Moad, *Polym. Chem.*, 2017, **8**, 177–219.
47 M. J. Monteiro and H. de Brouwer, *Macromolecules*, 2001, **34**, 349–352.
48 C. Barner-Kowollik, J. F. Quinn, D. R. Morsley and T. P. Davis, *J. Polym. Sci., Part A: Polym. Chem.*, 2001, **39**, 1353–1365.
49 S. W. Prescott, M. J. Ballard, E. Rizzardo and R. G. Gilbert, *Aust. J. Chem.*, 2002, **55**, 415–424.
50 K. H. Wong, T. P. Davis, C. Barner-Kowollik and M. H. Stenzel, *Polymer*, 2007, **48**, 4950–4965.
51 A. Goto, K. Sato, Y. Tsujii, T. Fukuda, G. Moad, E. Rizzardo and S. H. Thang, *Macromolecules*, 2001, **34**, 402–408.
52 P. B. Zetterlund, G. Gody and S. Perrier, *Macromol. Theory Simul.*, 2014, **23**, 331–339.
53 C. H. Hornung, X. Nguyen, S. Kyi, J. Chiefari and S. Saubern, *Aust. J. Chem.*, 2013, **66**, 192–198.
54 J. A. Balmer, S. P. Armes, P. W. Fowler, T. Tarnai, Z. Gáspár, K. A. Murray and N. S. Williams, *Langmuir*, 2009, **25**, 5339–5347.
55 D.-J. Liaw, K.-L. Wang and F.-C. Chang, *Macromolecules*, 2007, **40**, 3568–3574.
56 S. Kappaun, S. Horner, A. M. Kelterer, K. Waich, F. Grasse, M. Graf, L. Romaner, F. Niedermair, K. Müllen and A. C. Grimsdale, *Macromol. Chem. Phys.*, 2008, **209**, 2122–2134.
57 W. Sun, W. Tian, Y. Zhang, J. He, S. Mao and L. Fang, *Nanomedicine*, 2012, **8**, 460–467.
58 J. Raula, H. Eerikäinen and E. I. Kauppinen, *Int. J. Pharm.*, 2004, **284**, 13–21.
59 S.-P. Wen, J. G. Saunders and L. A. Fielding, *Polym. Chem.*, 2020, **11**, 3416–3426.
60 Y. Ning, L. A. Fielding, L. P. Ratcliffe, Y.-W. Wang, F. C. Meldrum and S. P. Armes, *J. Am. Chem. Soc.*, 2016, **138**, 11734–11742.
61 R. Gibson, S. Armes, O. Musa and A. Fernyhough, *Polym. Chem.*, 2019, **10**, 1312–1323.
62 E. Pedraza and M. Soucek, *Polymer*, 2005, **46**, 11174–11185.
63 F. S. Bates and G. H. Fredrickson, *Annu. Rev. Phys. Chem.*, 1990, **41**, 525–557.
64 M. W. Matsen and F. S. Bates, *Macromolecules*, 1996, **29**, 1091–1098.
65 L. Zha, J. Hu, C. Wang, S. Fu and M. Luo, *Colloid Polym. Sci.*, 2002, **280**, 1116–1121.
66 A. Drechsler, A. Synytska, P. Uhlmann, M. M. Elmahdy, M. Stamm and F. Kremer, *Langmuir*, 2010, **26**, 6400–6410.
67 S. North, E. Jones, G. Smith, O. Mykhaylyk, T. Annable and S. Armes, *Langmuir*, 2017, **33**, 1275–1284.
68 E. R. Jones, M. Semsarilar, A. Blanazs and S. P. Armes, *Macromolecules*, 2012, **45**, 5091–5098.
69 T. W. Healy, A. Homola, R. O. James and R. J. Hunter, *Faraday Discuss. Chem. Soc.*, 1978, **65**, 156–163.
70 D. Sato, M. Kobayashi and Y. Adachi, *Colloids Surf., A*, 2005, **266**, 150–154.

